Evidence for Specific Complex Formation between α-Melanocyte Stimulating Hormone and 6(R)-L-Erythro-5,6,7,8-tetrahydrobiopterin using Near Infrared Fourier Transform Raman Spectroscopy†

Jeremy Moore, John M. Wood, and Karin U. Schallreuter*

Clinical and Experimental Dermatology, Department of Biomedical Sciences, University of Bradford, West Yorkshire, BD7 1DP, United Kingdom

Received June 23, 1999; Revised Manuscript Received August 27, 1999

ABSTRACT: The cofactor 6(R)-L-erythro-5,6,7,8-tetrahydrobiopterin ($6BH_4$) and its 2 and 4 electron oxidation products 7,8-dihydro-L-biopterin and L-biopterin have been shown to form 1:1 complexes with the thirteen amino acid peptide α-melanocyte stimulating hormone (α-MSH). Hydrogen bonding to the pyrimidine ring of the cofactor has been established for glu[5] and his[6] of the hormone using Near Infrared Fourier Transform Raman spectroscopy. Binding of these pterins primarily involves the pyrimidine ring, although with the reduced pterins, 7,8-dihydro-L-biopterin and $6BH_4$, there is evidence for π orbital interaction with the pyrazine ring. It is proposed that this π orbital interaction with the reduced biopterins and α-MSH could provide the basis for the observed stability of these pterins to oxidation by either molecular oxygen or photooxidation by UVB (290−320 nm) light. Our results suggest that the formation of the α-MSH/$6BH_4$ complex could play a major role in the control of all $6BH_4$ dependent processes.

6(R)-L-erythro-5,6,7,8-tetrahydrobiopterin ($6BH_4$)[1] is the natural cofactor for the amino acid hydroxylases phenylalanine hydroxylase (PAH, EC 1.14.16.1), tyrosine hydroxylase (TH, EC 1.14.16.2) and tryptophan hydroxylase (TrpOH, EC 1.14.16.4) (*1*). $6BH_4$ also serves as cofactor for the nitric oxide synthases (NOS) (*2*). The aromatic amino acid hydroxylases share significant sequence homology and tertiary structure as well as conserved $6BH_4$ binding domains (*3*, *4*). During the catalytic cycle with the aromatic amino acid hydroxylases, $6BH_4$ undergoes a two electron oxidation to quinonoid dihydrobiopterin (qBH_2) via the proposed intermediate 4a-carbinolamine tetrahydrobiopterin (*5*). Quinonoid dihydrobiopterin spontaneously rearranges to 7,8-dihydro-L-biopterin (BH_2) and this product as well as L-biopterin exhibit no cofactor activity representing dead end byproducts in the catalytic cycle (*6*). In this context, it is interesting that BH_2 was used as a probe to identify the $6BH_4$ binding domain on TH by 500 MHz ^{1}H NMR spectroscopy (*7*).

Recently, it has been shown that epidermal cells (melanocytes and keratinocytes) have the full capacity for *de novo* synthesis, regulation, and recycling of $6BH_4$ (*8*). However, the presence of fully oxidized $6BH_4$ (i.e., L-biopterin), represents a rare event under physiological conditions. To our knowledge, it has only been detected in the epidermis of patients with the depigmentation disorder vitiligo (*9*). In vivo and in vitro studies of this condition have shown the accumulation of epidermal hydrogen peroxide (H_2O_2), in association with a perturbed $6BH_4$ recycling and inhibition of PAH leading to a build up of total L-phenylalanine in the epidermis of these patients (*10*, *11*). The oxidation of $6BH_4$ with H_2O_2 can yield several oxidation products depending on the reaction conditions such as BH_2, L-biopterin, sepiapterin, xanthopterin, and pterin (*12*).

It has been demonstrated that L-biopterin, xanthopterin, and sepiapterin are cytotoxic to melanocytes under in vitro conditions (*8*, *13*). Subsequently, it was discovered that $6BH_4$ regulates tyrosinase (EC 1.14.18.1), the key enzyme for melanogenesis, by uncompetitive allosteric inhibition (*14*). The $6BH_4$/tyrosinase inhibitor complex can be reactivated by α-melanocyte stimulating hormone (α-MSH) by 1:1 complexation with $6BH_4$ (*15*). The stoichiometry for this control mechanism was established by following radiolabeled [^{3}H] $6BH_4$ transfer from tyrosinase to α-MSH (*15*). Melanogenesis takes place in melanocyte specific organelles—the melanosomes. It is noteworthy that the presence of α-MSH has been confirmed in these organelles (*16*). Furthermore, we were able to show that α-MSH can also reactivate $6BH_4$ inhibited PAH (*11*). On the basis of these observations, it was postulated that α-MSH can play an important role in the regulation of both the intercellular formation of L-tyrosine from L-phenylalanine as well as the activity of tyrosinase in controlling melanogenesis (*17*, *18*).

Attempts to determine the structure of the $6BH_4$/α-MSH complex by X-ray crystallography or 2D 500 MHz ^{1}H NMR have failed so far (unpublished results). This is due to the instability of $6BH_4$ in solution under crystallizing conditions

* To whom correspondence should be addressed. Telephone: +44-1274-235529. Fax: +44 1274 235290. E-mail: K.Schallreuter@bradford.ac.uk.

† This research has been generously funded by Stiefel International with a grant to KUS.

[1] Abbreviations: ACTH, adrenocorticotropic hormone; α-MSH, alpha melanocyte stimulating hormone; BH_2, 7,8-dihydro-L-biopterin; $6BH_4$, 6(R)-L-erythro-5,6,7,8-tetrahydrobiopterin; glu, glutamic acid; GTP CH I, GTP cyclohydrolase I; his, histidine; met, methionine; NOS, Nitric oxide synthase; PAH, Phenylalanine hydroxylase; PTPS, Pyruvoyl tetrahydropterin synthase; qBH_2, quinonoid dihydrobiopterin; TH, Tyrosine hydroxylase; trp, tryptophan; TrpOH, Tryptophan hydroxylase; tyr, tyrosine.

10.1021/bi991448j CCC: $18.00
Published on Web 10/29/1999

A Acetyl-Ser[1]-Tyr[2]-Ser[3]-Met[4]-Glu[5]-His[6]-Phe[7]-Arg[8]-Trp[9]-Gly[10]-Lys[11]-Pro[12]-Val[13]-NH_2

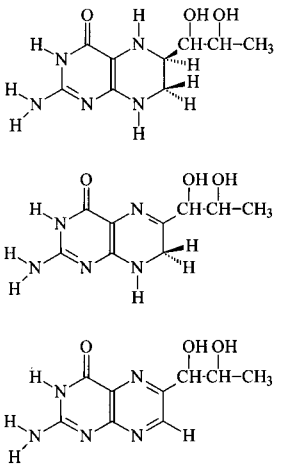

FIGURE 1: (A) Amino acid sequence of α-melanocyte stimulating hormone. (B, C, and D) Chemical structures of 6(R)-L-erythro-5,6,7,8-tetrahydrobiopterin, 7,8-dihydro-L biopterin, and L-biopterin.

and to self-association of this peptide under the concentration conditions required for the NMR experiments. In this context, it is noteworthy that X-ray crystallography of the ACTH peptide 4−10 (residues 4−10 of α-MSH) revealed that this peptide crystallized as a nonbiological structure with considerable self-association (*19*). Consequently, Fourier Transform Raman Spectroscopy (FT-Raman spectroscopy) has been utilized for the detailed study of the 1:1 $6BH_4$/α-MSH complex without sample degradation as this technique requires limited sample handling and works equally well for both the solid state and for complexes in solution. This paper presents for the first time a full FT-Raman spectral assignment of $6BH_4$, BH_2, and L-biopterin, α-MSH, and the $6BH_4$/α-MSH complex and the analogous complexes with BH_2 and L-biopterin. The sequence for α-MSH and the structures for $6BH_4$, BH_2, and L-biopterin are presented in Figure 1.

MATERIALS AND METHODS

FT-Raman spectra were acquired using a Bruker RFS 100/S spectrometer with a liquid nitrogen cooled Germanium detector. Near infrared excitation was produced by a Nd^{3+}:YAG laser operating at 1064 nm. Individual spectra were accumulated over 6000 scans with a resolution of 4 cm^{-1}. Spectra were normalized using the mono substituted aromatic ring breathing vibration of the phenylalanine residue located at 1004.1 cm^{-1} and were corrected automatically for instrument response without employment of baseline correction techniques.

Synthetic α-MSH (95% purity) was obtained from Sigma Chemical Company, Dorset, UK. High purity 6(R)-L-erythro-5,6,7,8-tetrahydrobiopterin 7,8-dihydrobiopterin, and L-biopterin were obtained from Schircks Laboratories, Jona, Switzerland. Solid samples of the peptide/pterin complexes were produced by mixing equimolar amounts of both peptide and cofactor followed by immediate lyophilisation using an Edwards freeze-dryer. The pH of each solution was adjusted to pH 5.5 using an Orion micro pH probe. Dried samples were stored at −80 °C prior to FT-Raman spectrum acquisition.

RESULTS

Previous Raman spectroscopic work on pterin and folate cofactors has centered on individual interactions with specific functional groups on these cofactor molecules (*20*, *21*). Assignments for the in-plane normal modes for isoxanthopterin and lumazine have also been produced using Resonance Raman spectroscopy (*22*). However, to date, there has not been a full Raman spectroscopic assignment of pterins in their different redox states.

Raman Spectra of $6BH_4$, BH_2, and L-Biopterin. The pterin ring system gives rise to vibrations that correspond to each six-membered pyrimidine and pyrazine ring. Both rings produce in and out of plane deformation modes (500−700 cm^{-1}), in phase ring bends (950−1000 cm^{-1}), and ring quadrant stretches (1470−1600 cm^{-1}). The individual functional groups are assigned in Table 1 and Figures 2, a, b, and c. The side chain of all the biopterins examined produces weak aliphatic vibrations that have not been characterized in this study due to their relatively weak Raman scattering and hence lack of visibility in the biopterin/α-MSH complex spectra.

FT-Raman Spectrum of Free α-MSH. α-MSH yields characteristic Raman vibrations for 6 of the 13 amino acid side chain functional groups. The predominant vibrations are seen for the aromatic amino acids phenylalanine, tyrosine, tryptophan, and the imidazole ring of histidine as well as conformation dependent vibrations for methionine and the carboxylic acid group of glutamic acid (Table 2). Additionally, the peptide backbone produces two different coupled resonances—amide I and amide III. The amide I vibration is predominantly the carbon−oxygen stretch vibration coupled with the nitrogen−hydrogen stretch, the amide III is the carbon−nitrogen stretch coupled with the nitrogen−hydrogen bending mode. The amide III is considerably more sensitive to hydrogen bonding in the backbone (i.e., interpeptide hydrogen bonds), whereas the amide I shows a similar response to the amide III but is more a feature of the backbone conformation produced by the interpeptide hydrogen bonds. The FT-Raman spectrum of uncomplexed α-MSH has a clearly resolved amide I vibration located at 1671.7 cm^{-1} (Figure 3) (Table 2). Amide I vibrations at this wavenumber are consistent with a random structure with no ordered conformation (*23*). The lack of the ordered conformation is supported by the absence of the amide III vibration, with no interpeptide hydrogen bonds. This observation is in agreement with preliminary 500 MHz ^1H NMR data, which also indicate that the peptide has no ordered structure in solution. The phenylalanine aromatic ring breathing vibrations are least affected upon 1:1 complexation of α-MSH to $6BH_4$, yielding little or no intensity change or shift in all cases. On the basis of this observation, these vibrational modes associated with phenylalanine could be used as reference peaks for other spectral assignments.

Spectral Assignments for the $6BH_4$, BH_2, and L-Biopterin/α-MSH Complexes. FT-Raman Assignments for the 500−1150 cm^{-1} Region. The biopterin molecules produce vibrations specific to the two heterocyclic pyrimidine and pyrazine rings. Upon complexation to α-MSH, the pterin molecule reveals ring deformation modes located in the region 500−700 cm^{-1}. The in-plane deformation mode for the pyrimidine

Table 1: FT-Raman Assignments for 6(R)-L-Erythro-5,6,7,8-tetrahydrobiopterin ($6BH_4$), 7,8-Dihydro-L-biopterin (BH_2), and L-Biopterin[a]

assignment	L-biopterin	BH_2	$6BH_4$
C═O	1686.7		1687.5
NH_2 scissors bending	1649.4	1644.2	1659.3
			1639.2 (sh)
C═N		1627.2(sh)	
			1619.5
		1607.9	
	1600.0 (sh)		
			1597.4
pyrimidine ring quadrant stretch	1582.2	1589.8	1574.4
pyrimidine ring quadrant stretch	1537.9	1560.9	
saturated pyrazine ring stretch			1527.1
pyrazine ring quadrant stretch	1513.9		
pyrazine ring quadrant stretch	1480.9	1472.0	1473.8
terminal CH_3	1457.5	1443.5	1454.9
C−OH deformation	1423.4	1402.2	1403.7
			1389.6
pyrimidine ring semicircle stretch	1371.6		1361.5
6-position C−C bend	1349.6	1352.0	
C−H in plane bending (7-position)	1323.3	1321.6	1331.0
	1301.0 (sh)	1306.3	1310.0
C−H out of plane bending (7-position)	1288.4	1251.3	1226.0
		1208.8	
C−C coupled resonance with C−OH	1173.9	1172.2	1173.8
	1130.3	1129.1	1130.3
			1115.9
		1109.8	1109.4
	1093.0	1089.4	1093.0
	1079.9	1081.2	1079.9
	1060.2		1060.2
	1045.5	1043.9	1047.1
		1026.7	
	1006.1		1006.1
alkyl substituted pyrazine in phase ring bend	976.3		
pyrazine ring out of phase ring bend	959.3		
		948.0	
	939.4		
	928.7		
	888.9		881.6
	870.1	877.9	
			861.1
	831.1		
		823.6	
			811.1
	798.0		
		779.5	
	753.7		
			742.6
		730.3	
			717.6
pyrimidine ring out of plane deformation	694.2	705.7	690.9
pyrazine ring out of plane deformation	665.0	667.1	643.7
	603.7		
	594.5		593.2
		557.6	551.2
pyrimidine in plane deformation	539.5	538.2	535.5
	521.9		
pyrazine in plane deformation	509.3	513.9	515.2
			503.3

[a] (sh = shoulder).

ring is observed at 540 ± 4 cm^{-1} and is clearly independent of the biopterin redox status (Figure 4 and Table 3). The pyrazine ring in plane deformation mode is located at 509.2 cm^{-1} for L-biopterin, 513.9 cm^{-1} for BH_2, and 515.2 cm^{-1} for $6BH_4$. The change in position of this vibrational mode is most likely due to the different redox status that controls the flexibility of the pyrazine ring. The out of plane deformation mode of the pyrazine ring at 664.5, 673.8, and 643.7 for L-biopterin, BH_2, and $6BH_4$, respectively, is affected by the heteroaromaticity of the ring, resulting in a shift in peak position. This is the most intense peak for all of the biopterin spectra.

The pyrimidine ring out of plane deformations are all located at a 30 cm^{-1} higher wavenumber than the corresponding pyrimidine ring deformation at 694.2, 705.7, and 690.9 for L-biopterin, BH_2, and $6BH_4$, respectively. Upon complexation to α-MSH, the pyrimidine ring vibration of $6BH_4$ decreases in intensity in comparison to the pyrazine ring. This is a clear indication that the hydrogen bond formation between the glu^5, his^6, and the pyrimidine ring

Table 2: FT-Raman Assignments for α-Melanocyte Stimulating Hormone Residues and Functional Groups[a]

residue/molecule	vibration	α-MSH
protein backbone (C═O)	amide I	1671.7
tyr	ring stretch	1616.2
phe	ring stretch	1605.3
trp	indole ring stretch	1583.5
trp	indole ring stretch	1550.7
		1518.1
		1489.4
aliphatic R groups	CH_2 scissor	1456 (sh)
glu	COO^-	1440.4
glu	COO^-	1428.1 (sh)
trp	exposed ring deformation	1356.9
trp		1339.1
protein backbone	amide III	1311
		1279
his	(tautomer 2 N_3−H)	1250.0
his	(tautomer 1 N_1−H)	1235.2
tyr		1206.7
phe/tyr		1175.4
		1127.7
		1051.5
phe	2,4,6 quadrant ring breathing	1032.4
phe	1,3,5 quadrant ring breathing	1004.3
		929 (sh)
		919.9
trp		877.7
tyr	OH group free	853.5
tyr	OH group bound	828
trp		759.0
met	C−S (trans)	721
met	C−S (cis)	702
tyr	ring deformation	642
phe	ring deformation	623

[a] (sh = shoulder).

restricts movement of the bound $6BH_4$. As the pyrimidine ring is restricted, it can no longer undergo the deformation mode needed to produce a Raman vibration. Hence, there is a major reduction in the intensity of this peak in the Raman spectrum. The same effect is seen to a lesser extent in the spectrum of the BH_2 complex. However, the L-biopterin complex spectrum shows no change in the pyrimidine ring vibration intensity, probably due to the extended conjugation of the pyrimidine and pyrazine rings of the fully oxidized L-biopterin.

Inspection of the in-plane deformation modes of the pyrazine ring (500−570 cm^{-1}) reveals a novel feature upon complexation. $6BH_4$ and BH_2 both present new features at a lower wavenumber compared to the uncomplexed state (i.e., 502.7 and 495.8 cm^{-1}). L-biopterin has a new peak at a higher wavenumber (i.e., 523.6 cm^{-1}). The varying wavenumber of these new features underlines that the binding of $6BH_4$ and BH_2 to α-MSH produces similar constraints on the biopterin molecules, whereas the effects of binding to the L-biopterin molecule are different. This change in binding may well arise from the aromaticity of the L-biopterin, producing a variation in charge within the binding site leading to subtle differences for the α-MSH-cofactor interaction.

The phenylalanine residue produces three peaks, one ring deformation mode at 623.4 cm^{-1} and two trigonal ring breathing bands at 1032.4 and 1004.1 cm^{-1}, which are all unaffected by complexation to any of the biopterins. As with phenylalanine, tyrosine produces three peaks in this region, the ring deformation at 642.3 cm^{-1} and the hydrogen bond

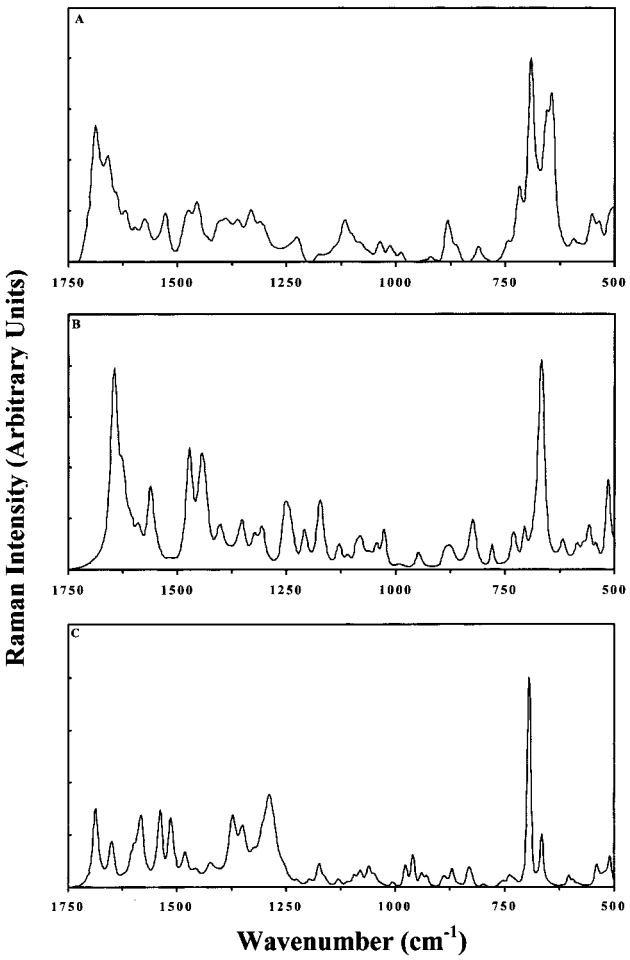

FIGURE 2: FT-Raman spectra (500−1750 cm^{-1}) of: (A) 6(R)-L-erythro-5,6,7,8-tetrahydrobiopterin, (B) 7,8-dihydro-L-biopterin, and (C) L-biopterin.

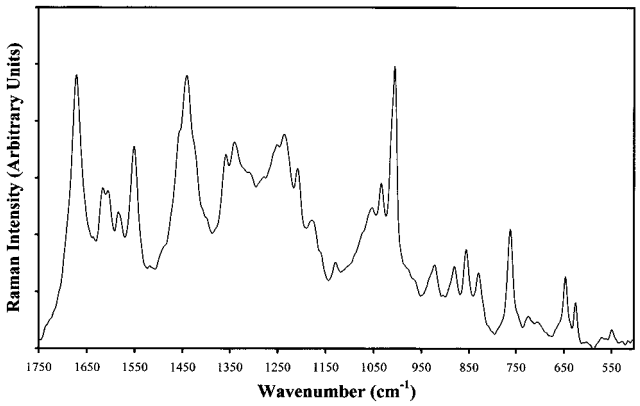

FIGURE 3: FT-Raman spectrum (500−1750 cm^{-1}) of uncomplexed α-MSH.

sensitive doublet at 853.5 and 828.4 cm^{-1} (*24*). The ring deformation mode is obscured by the $6BH_4$ spectrum, but it is clearly visible in both the L-biopterin and BH_2 spectra. A comparison of the same vibrational mode for phenylalanine and tyrosine shows a decrease in intensity between the L-biopterin complex and the BH_2 complex. The tyr^2 free hydroxyl group peak of the hydrogen bond sensitive doublet undergoes no change unlike the bound hydroxyl group peak, which increases in intensity in the presence of L-biopterin and BH_2. However, there are corresponding peaks in the spectrum of both L-biopterin and BH_2, which overlap this

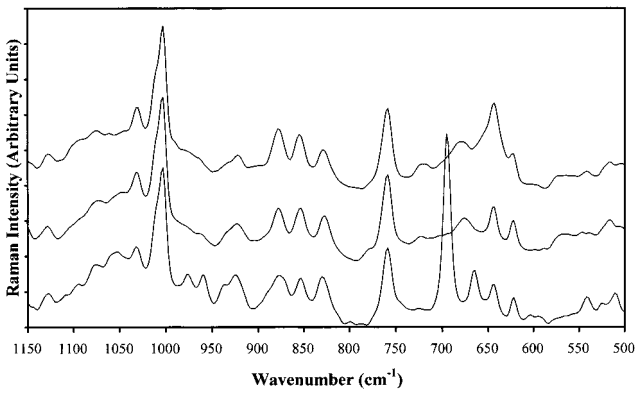

FIGURE 4: Stack plotted FT-Raman spectra (500−1150 cm^{-1}) of α-MSH complexed with 6(R)-L-erythro-5,6,7,8-tetrahydrobiopterin (top), 7,8-dihydro-L-biopterin (middle), and L-biopterin (bottom).

tyrosine residue vibration, and so it remains unclear whether there is any major change in this vibrational mode of tyr^2 upon complex formation. The $6BH_4$ complex shows no change in this tyr^2 peak and has no overlapping bands in this area.

The tryptophan residue produces two vibrational modes at 758.7 and 877.7 cm^{-1}. The 758.7 cm^{-1} peak remains unaltered on complexation, while the aromatic carbon−hydrogen wag of the indole ring of tryptophan gives rise to a single vibrational mode located at 877.7 cm^{-1}. Upon examination of all the α-MSH/biopterin complexes, this vibrational mode appears to increase in all cases. The results show that L-biopterin has two peaks at 870.1 and 888.9 cm^{-1}, which clearly overlap this vibrational mode for tryptophan, but none of these overlapping peaks are present in the spectrum of BH_2 or $6BH_4$. In addition, the increase is greater in the $6BH_4$ complex than the BH_2 complex, indicating a greater structural perturbation on α-MSH upon complexation to the fully reduced active form of this cofactor.

The carbon−sulfur−carbon bond of methionine in the α-MSH sequence produces a weak doublet consistent with a mixed orientation of this bond between trans and cis at 721.2 and 702.7 cm^{-1}, respectively. In the uncomplexed form of α-MSH, the methionine is mainly in the trans conformation. There is no change in the peak intensity of the trans form of methionine on complexation, however, the cis peak is obscured in all cases.

FT-Raman Assignments for the 1150−1750 cm^{-1} Region. This region contains the most information with regard to the peptide structure in the amide I and III bands. Uncomplexed α-MSH has a single peak in the amide I area at 1671.7 cm^{-1}, which correlates with an unordered/random confirmation. After complexation with BH_2 and $6BH_4$, several new features are observed at 1635.3, 1641.6, and 1649.2 cm^{-1} (Figure 5). These new peaks represent additional amide I vibrations and fit a structure commonly described as a β-turn (i.e., 1641.6 cm^{-1}) and α-helices (i.e., 1635.3 and 1649.2 cm^{-1}). Both of the α-helical vibrations are found as shoulders on the main β-turn peak with increasing intensity from BH_2 to $6BH_4$, whereas the β-turn peak decreases in intensity, indicating a change in the peptide conformation on complexation with $6BH_4$. The unordered amide I vibration remains unchanged with L-biopterin but decreases with BH_2 and $6BH_4$, with the most pronounced decrease in the $6BH_4$/α-MSH complex. The two shoulders on the amide I vibration of the L-biopterin complex spectrum are consistent with a carbonyl carbon−oxygen stretch (i.e., 1686.7 cm^{-1}) and an amine group NH_2 scissoring mode (i.e., 1649.4 cm^{-1}). The amide III vibrations support the observations from the amide I region with the production of new peaks matching those from the amide I region. For the L-biopterin/α-MSH complex the α-helical vibration is found at 1331.3 cm^{-1}. The β-turn vibration is found at 1305.1 cm^{-1}. In the latter complex, there is again an overlapping band at 1288.4 cm^{-1} from the pyrazine ring aromatic C−H bending mode.

The carboxylic acid group of glutamic acid in α-MSH produces distinctive vibrations dependent on the ionization state of the carboxylate group. In the uncomplexed form, this remains unionized as a weak shoulder at 1428.1 cm^{-1} with a coupled resonance of the carbon−oxygen double bond and the carbon−oxygen single bond at 1456.3 cm^{-1}. L-biopterin complexation uncouples the two carbonyl group resonances, resulting in a decrease in this coupled resonance vibration. However, with BH_2 and $6BH_4$ complexation, the unionized vibration disappears, while a new ionized vibration occurs at 1471.8 cm^{-1}. With $6BH_4$ complexation, both the ionized and coupled resonance's increase in comparison to the BH_2 spectrum implicating strong interaction between glu^5 in α-MSH and the $6BH_4$ molecule.

In addition to the glu^5 being directly involved in binding, the imidazole ring of the histidine residue at position 6 can also be studied as it undergoes tautomerisation upon complexation. Prior to complex formation, the imidazole ring is predominantly protonated at the N_3 (1235.2 cm^{-1}) (tautomer I), which switches to predominantly N_1 protonation (1250.0 cm^{-1}) (tautomer II) when biopterin/α-MSH complexes are formed (*25*).

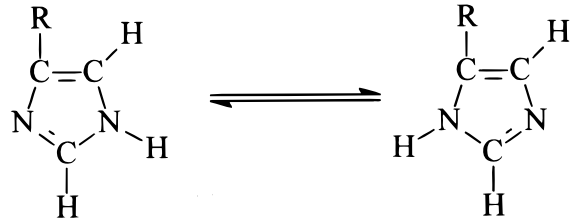

Tautomer I Tautomer II

Both tautomer peaks increase dramatically in intensity when complexed to BH_2 but decrease with $6BH_4$. This unusual intensity increase can be attributed to a closer binding of the pterin molecule to the imidazole ring with subsequent shortening of the nitrogen−hydrogen bond. The fact that the intensity decreases to almost normal levels with the $6BH_4$ complex strongly indicates that the binding of α-MSH to $6BH_4$ primarily involves the glu^5 residue with a weaker interaction with his^6. This difference can be accounted for as the histidine residue has a greater attraction to BH_2.

Interactions with the trp^9 indole ring can be observed at 1356.2 cm^{-1}. An increase in this peak is seen upon L-biopterin complexation to α-MSH and is characteristic for the indole ring being buried in the peptide structure (*26*). The opposite is seen with BH_2 where the peak decreases as

Table 3: FT-Raman Assignments for α-Melanocyte Stimulating Hormone Complexes with L-Biopterin, 7,8-Dihydro-L-biopterin (BH_2), and 6(R)-L-Erythro-5,6,7,8-tetrahydrobiopterin ($6BH_4$)[a]

residue/molecule	vibration	L-biopterin/α-MSH	BH_2/α-MSH	$6BH_4$/α-MSH
biopterin	C═O	1685		
protein backbone	amide I	1670.8	1669.0	1668.3
biopterin/$6BH_4$	NH_2 scissor	1650 (sh)		1657.0
				1649.2
			1640.4	1641.6
				1635
tyr	ring stretch	1615.6	1619.4	1618.5
phe	ring stretch	1604.1	1606.9	
trp	indole ring stretch	1582.5	1582.8	1583.7
trp	indole ring stretch	1549.1	1551.3	1551.7
biopterin	pyrazine quadrant ring stretch	1539 (sh)		
		1514.3		1515.1
		1479 (sh)	1475.3	1471.8
aliphatic R groups	CH_2 scissor	1456	1457	1457.8
glutamic acid	COO^-	1440.7	1441.9	1443.0
glutamic acid	COO^-	1426 (sh)		
			1408.1	
$6BH_4$	pyrimidine ring semicircle stretch			1392.4
$6BH_2$	pyrimidine ring semicircle stretch		1383.5	
biopterin	pyrimidine ring semicircle stretch	1372 (sh)		
trp	exposed ring deformation	1357	1357	1356.2
trp		1344.1	1339.3	1339.7
protein backbone	amide III		1317.4	
	amide III	1302	1304.2	1305.1
biopterin	heteroaromatic C−H bending (7-position)	1287.8		
			1281.9	
his	(tautomer 2 N_3−H)	1255.9	1251.0	1251.9
his	(tautomer 1 N_1−H)	1238	1236	1238
tyr		1207.7	1206.9	1206.4
			1182.9	
phe/tyr		1173.5	1173.3	1179.9
			1158.5	1159.4
		1128.1	1127	1128.2
		1052.8		
phe		1032.1	1031.9	1031.2
phe		1003.7	1003.7	1003.4
			983.5	
biopterin	pyrazine in phase ring bend	976.8		
biopterin	pyrazine out of phase ring bend	959.7		
biopterin	pyrimidine in phase ring bend	937		
		924.5	925.6	922.0
				897.2
trp		876.7	877.2	877.2
tyr	OH group free	853.3	854.1	854.4
tyr	OH group bound	829.6	827.1	828.3
trp		758.6	758.6	758.7
met	C−S (trans)		722	720.5
met	C−S (cis)			
	pyrimidine in plane ring deformation	694.2	694	
biopterin/BH_2/$6BH_4$	pyrazine ring in plane deformation	664.5	673.8	677.8
tyr	ring deformation	643.6	643.4	643.1
phe	ring deformation	621.5	621.8	622.6
biopterin		602.7		
biopterin		594		
BH_2			571.7	571.8
BH_4				563.6
BH_4				555.8
biopterin/BH_2/$6BH_4$	pyrimidine in plane ring deformation	540.2	543.6	540.4
biopterin/BH_2/$6BH_4$	pyrazine in plane deformation	509.2	513.9	515.2
BH_4				502.9

[a] (sh = shoulder).

the indole ring is exposed to the medium. $6BH_4$ causes the peak to decrease to a lesser extent than BH_2, suggesting that BH_2 interaction with the indole ring is weaker than with $6BH_4$. This trend is again repeated in the otherwise insensitive indole ring stretch at 1551.7 cm^{-1} where the peak increases in the BH_2 and $6BH_4$ complexes with the biggest increase seen in the BH_2 complex. The out of phase carbon−carbon double bond stretch band at 1583.7 cm^{-1} appears to be unaffected by BH_2/α-MSH complex formation but decreases in $6BH_4$/α-MSH compared to free α-MSH. The remaining indole ring vibration at 1339.7 cm^{-1} remains unaffected in all 3 biopterin complexes.

The tyrosine ring stretch at 1618.5 cm^{-1} decreases in comparison to the phenylalanine ring stretch at 1605.3 cm^{-1} in the L-biopterin complex but increases in both the BH_2 and $6BH_4$ complexes standardized to the α-MSH phenylalanine signal. This effect is more pronounced in the BH_2/α-MSH spectrum. The 1206.7 cm^{-1} tyrosine band also increases with complexation but there is very little difference between the BH_2/α-MSH and $6BH_4$/α-MSH complexes.

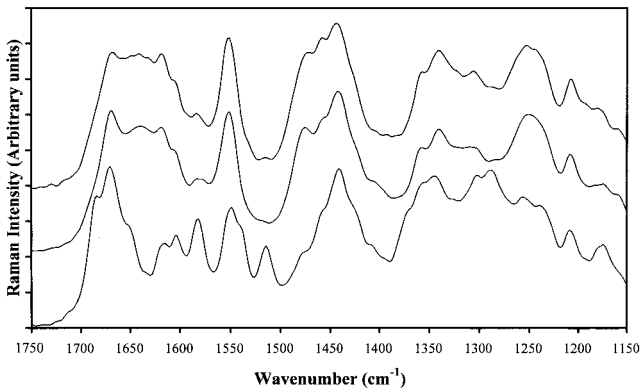

FIGURE 5: Stack plotted FT-Raman spectra (1150−1750 cm^{-1}) of α-MSH complexed with 6(R)-L-erythro-5,6,7,8-tetrahydrobiopterin (top), 7,8-dihydro-L-biopterin (middle), and L-biopterin (bottom).

DISCUSSION

$6BH_4$ functions as an essential cofactor/electron donor for the aromatic amino acid hydroxylases PAH, TH, and TrpOH as well as for all nitric oxide synthases (*1*, *2*). Therefore, this cofactor plays a crucial role in controlling the synthesis of neurotransmitters, such as catecholamines, serotonin, and nitric oxide (*2*, *27*). In addition, $6BH_4$ has been identified as an uncompetitive/allosteric inhibitor of tyrosinase, the key enzyme for melanogenesis (*14*). Experiments with ^{3}H-labeled $6BH_4$ established a 1:1 stoichiometry for α-MSH/$6BH_4$ complexation in the activation of tyrosinase (*16*). Studies with α-MSH and other ACTH-related peptides indicated that complex formation between $6BH_4$ and α-MSH is specific since neither ACTH (1−39) nor desacetyl MSH (i.e., ACTH 1−13) bind $6BH_4$ nor activate tyrosinase (*14*, *17*). Furthermore, substitution of glu^5 with ala^5 in α-MSH causes the peptide to lose its ability to bind $6BH_4$ and to activate tyrosinase (*14*). Examination of truncated peptides of α-MSH revealed that the tripeptide met^4−glu^5−his^6 showed approximately 20% of the activity of α-MSH in the tyrosinase assay (*16*, *17*). Hyperchem modeling of the $6BH_4$/α-MSH complex support a structure involving H-bonds from the N-acetyl group of ser^1, two H-bonds from glu^5, one from his^6 and one from the peptide bond of val^{13} (*16*, *17*). However, in the absence of X-ray crystallographic data on the three-dimensional structure of the complex, attempts to model the $6BH_4$/α-MSH interaction remain speculative. Therefore, in this study FT-Raman spectroscopy was utilized to examine both the structure of free α-MSH and its 1:1 complexes with $6BH_4$, BH_2, and L-biopterin. Both 500 MHz ^{1}H NMR and FT-Raman spectroscopy established that free α-MSH has a random structure in solution (unpublished NMR results). The results of this study show that the α-MSH interaction with L-biopterin, BH_2, and $6BH_4$ occurs via hydrogen bond formation between the protonated nitrogen (N_1) of the imidazole ring of his^6 and through the carbonyl groups of the carboxylic acid functional group of glu^5. Because of the close proximity of these two residues in the α-MSH sequence at positions 5 and 6 and the specific requirements for the formation of the hydrogen bonds, there are considerable constraints for binding to the pterin ring system. Upon α-MSH complex formation with $6BH_4$, the pyrimidine ring is also severely restricted in its deformation mode. Taken together, these results clearly identify the importance of the pyrimidine ring in complex formation. In this context, it is noteworthy that X-ray crystallographic results on GTP cyclohydrolase I (GTP−CH I) and pyruvoyl tetrahydropterin synthase (PTPS) have both produced binding domains in their respective proteins that include pyrimidine ring anchoring via a glutamic acid residue (*28*, *29*). GTP−CH I also has a basic lysine residue that hydrogen bonds to the carbonyl group of the pyrimidine ring where the glutamic acid and lysine are adjacent to each other in positions 151 and 152, respectively. A similar scenario is true for PTPS. Here is an identical reaction with glu^{107} and a hydrogen bond from the N−H of the peptide bond between thr^{105} and thr^{106} (*29*). On the basis of the similar binding domains of GTP−CH I and PTPS, we would like to conclude that the structure of the α-MSH complexes with $6BH_4$ and BH_2 involves glu^5 anchoring of the pyrimidine ring by hydrogen bonding at the C_2 amino group and the N_3 amide group. Furthermore, the N^1 tautomer of the his^6 residue forms a third hydrogen bond with the carbonyl group of the pyrimidine ring. The interaction of these two residues with the pyrimidine ring could well control the relative binding affinities of biopterins in their different oxidation states. This structure is supported by the observation that the carboxylate group of the glu^5 yields spectral differences depending on the redox status of the biopterins.

It is important to realize that L-biopterin binds weakly to the carbonyl group of glu^5 with a consequent loss of the coupled resonance and the formation of a single carbonyl group leaving an unionized carbon−oxygen−hydrogen bond. On the other hand, both BH_2 and $6BH_4$ do not uncouple this carboxylic acid resonance. A newly ionized carbonyl group is formed, indicating that the binding of BH_2 and $6BH_4$ proceeds via two similar carbonyl functions with a coupled resonance. This result suggests that the bond ionization is most likely shared between the two carbonyl groups in the same manner as seen for the unionized carboxylic acid group where the dipole moment is shared across the O−C−O bond. Despite BH_2 and $6BH_4$ binding to the glu^5 and his^6 in the same way, there is still evidence for different modes of binding for these two biopterins. BH_2 complexation produces a much more intense interaction with the his^6 than is observed with $6BH_4$. The latter interacts more strongly with glu^5. These differences in pyrimidine ring binding may well indicate the relative abilities of each of these compounds to form stable complexes with α-MSH. A comparison of BH_2 and $6BH_4$ with L-biopterin binding to α-MSH clearly shows that the decrease in heteroaromaticity of the pyrazine ring has a major influence on complex formation and this determines the redox status of the biopterins. The crucial question remains: how can the redox status of the molecule alter the ability of the pyrimidine ring to bind to the carboxylate group of glu^5?

The specificity for the fully reduced $6BH_4$ could be caused by factors other than a simple anchoring mechanism. Upon recent examination of X-ray crystallographic structures of the $6BH_4$ dependent enzymes TH and NOS (*3*, *30*, *31*), it was observed that both contain an aromatic amino acid residue (i.e., phenylalanine or tryptophan) planar to the $6BH_4$ molecule. This feature has been labeled as π stacking. In the α-MSH complex, the indole ring of the trp^9 is greatly perturbed. This perturbation may represent π stacking, which appears more as a π orbital interaction. This π orbital interaction would explain the observed stabilization to oxidation of $6BH_4$ by α-MSH upon complexation and also

the proposed stabilization of the $6BH_4$ cation radical proposed in the catalytic cycle of NOS (*15*, *31*). The secondary structure of the peptide is also greatly affected by complexation, where the unordered conformation gives way to a β-turn and two different α-helices. This β-turn at met[4] was predicted previously by the Hyperchem model of the $6BH_4$/α-MSH complex (*32*). As α-MSH has been shown to adopt a helical structure when associated with membranes, it is not surprising to note the formation of α-helices (*33*). However, in the $6BH_4$/α-MSH complex, the formation of a β-turn would not be consistent with any association studied so far for free α-MSH. In this context, it is interesting that analogues of α-MSH have been produced with D-phenylalanine in place of the L configuration, creating a β-turn like conformation in the peptide backbone, which have shown enhanced properties when assayed against the natural hormone (*34*).

In summary, the results of this study support the formation of a specific α-MSH/$6BH_4$ structure primarily involving interactions between the glu[5] and his[6] residues of the peptide and the pyrimidine ring of the biopterin molecule. In addition to this, a stabilizing π-orbital interaction between the indole ring of trp[9] and the pyrazine ring of the reduced forms of the biopterins studied has been proposed.

ACKNOWLEDGMENT

Helen Bartle typed the manuscript. J.M. acknowledges the support of Wayne Beazley for his encouragement and intellectual discussions.

REFERENCES

1. Hufton, S. E., Jennings, I. G., and Cotton, R. G. H. (1995) *Biochem. J. 311*, 353−366.
2. Kwon, N. S., Nathan, C. F., and Stuehr, D. J. (1989) *J. Biol. Chem. 264*, 20496−20501.
3. Goodwill, K. E., Sabatier, C., Marks, C., Raag, R., Fitzpatrick, P. F., and Stevens, R. C. (1997) *Nat. Struct. Biol. 4*, 578−585.
4. Fusetti, F., Erlandsen, H., Flatmark, T., and Stevens, R. C. (1998) *J. Biol. Chem. 273*, 16962−16967.
5. Davis, M. D., and Kaufman, S. (1989) *J. Biol. Chem. 264*, 8585−8596.
6. Archer, M. C., and Scrimgeour, K. G. (1970) *Can. J. Biochem. 48*, 278−287.
7. Martinez, A., Vageli, O., Pfleiderer, W., and Flatmark, T. (1998) *Pteridines. 9*, 44−52.
8. Schallreuter, K. U., Wood, J. M., Ziegler, I., Lemke, K. R., Pittelkow, M. R., Lindsey, N. J., Gütlich, M. (1994) *Biochim Biophys Acta 1226*, 181−92.
9. Schallreuter, K. U., Wood, J. M., Pittelkow, M. R., Gütlich, K., Lemke, R., Rödl, W., Swanson, N. N., Hitzemann, K., and Ziegler, I. (1994) *Science. 263*, 1444−1446.
10. Schallreuter, K. U., Zschiesche, M., Moore, J., Panske, A., Hibberts, N. A., Herrmann, F. H., Metelmann, H. R., and Sawatzki, J. (1998) *Biochem. Biophys. Res. Commun. 243*, 395−399.
11. Schallreuter, K. U., Moore, J., Wood, J. M., Beazley, W. D., Gaze, D. C., Tobin, D. J., Marshall, H. S., Panske, A., Panzig, E., and Hibberts, N. A. (1999) *J. Invest. Dermatol. Symp. Proc. 4*, 91−96.
12. Moore, J., Beazley, W. D., Wood, J. M., and Schallreuter, K. U. (1999) *Pteridines. 10*, 57.
13. Schallreuter, K. U., Büttner, G., Pittelkow, M. R., Wood, J. M., Swanson, N. N., and Körner, C. (1994) *Biochem. Biophys. Res. Commun. 204*, 43−48.
14. Wood, J. M., Schallreuter-Wood, K. U., Lindsey, N. J., Callaghan, S., and Gardner, L. G. (1995) *Biochem. Biophys. Res. Commun. 206*, 480−485.
15. Schallreuter, K. U., Moore, J., Jenner, T., Lindsey, N. J., Wood, J. M., Thody, A. J., and Graham. A. (1997) in *Chemistry and Biology of Pteridines and Folates.* (Pfleiderer, W., and Rokos, H., Eds.) pp791−795.
16. Schallreuter, K. U., Moore, J., Tobin, D. J., Gibbons, N. J. P., Marshall, H. S., Jenner, T., Beazley, W. D., and Wood, J. M. (1999) *Ann. N. Y. Acad. Sci. 885*, 329−341.
17. Lerner, A. B. (1980) *J. Invest. Dermatol. 75*, 121.
18. Wintzen, M., and Gilchrest, B. A. (1996) *J. Invest. Dermatol. 106*, 3−10.
19. Admiraal, G., and Vos, A. (1984) *Int. J. Pept. Protein Res. 23*, 151−157.
20. Kilpatrick, L., Rajagopalan, K. V., Hilton, J., Bastian, N. R., Stiefel, E. I., Pilato, R. S., and Spiro, T. G. (1995) *Biochemistry 34*, 3032−3039.
21. Chen, Y. Q., Kraut, J., Blakley, R. L., and Callender, R. (1994) *Biochemistry 33*, 7021−7026.
22. Brutovský, B., Ulicný, J., Miškovský, P., Lisý, V., and Chinsky, L. (1998) *J. Raman Spectrosc. 29*, 833−839.
23. Williams, R. W., Cutrera, T., Dunker, A. K., and Peticolas, W. L. (1980) *FEBS Lett. 115*, 306−308.
24. Siamwiza, N., Lord, R. C., Chen, M. C., Takamatsu, T., Harada, I., Matsuura, H., and Shimanouchi, T. (1975) *Biochemistry 14*, 4870−4876.
25. Ashikawa, I., and Itoh, K. (1979) *Biopolymers 18*, 1859−1876.
26. Tu, A. T., Jo, B. H., and Yu, N. T. (1976) *Int. J. Pept. Protein Res. 8* (*4*), 337−343.
27. Kaufman, S. (1997) *Tetrahydrobiopterin*, The John Hopkins University Press, Baltimore, MD.
28. Nar, H., Huber, R., Heizmann, C. W., Thöny, B., and Bürgisser, D. B. (1994) *EMBO J. 13*, 1255−1262.
29. Bürgisser, D. M., Thöny, B., Redweik, U., Hess, D., Heizmann, C. W., Huber, R., and Nar, H. (1995) *J. Mol. Biol. 253*, 358−369.
30. Crane, B. R., Arvai, A. S., Ghosh, D. K., Wu, C., Getzoff, E. D., Stuehr, D. J., and Tainer, J. A. (1998) *Science 279*, 2121−2126.
31. Raman, C. S., Li, H., Martasek, P., Kral, V., Masters, B. S., and Poulos, T. L. (1999) *Cell 95*, 939−50.
32. Moore, J., Wood, J. M., and Schallreuter, K. U. (1997) in *Chemistry and Biology of Pteridines and Folates.* (Pfleiderer, W. and Rokos, H., Eds.) pp 831−835.
33. Biaggi, M. H., Pinheiro, T. J., Watts, A., and Lamy-Freund, M. T. (1996) *Eur. Biophys. J. 24*, 251−259.
34. Cody, W. L., Mahoney, M., Knittel, J. J., Hruby, V. J., Castrucci, A. M., and Hadley, M. E. (1985) *J. Med. Chem. 28*, 583−588.

BI991448J